Adsorption (2020) 26:701–709
https://doi.org/10.1007/s10450-019-00147-w

A facile approach to the fabrication of MgO@Y composite for CO_2 capture

Fei Gao[1] · Shougui Wang[2] · Guanghui Chen[1] · Jihai Duan[1] · Jipeng Dong[1] · Weiwen Wang[1]

Received: 9 April 2019 / Revised: 3 July 2019 / Accepted: 8 July 2019 / Published online: 13 July 2019

Abstract
Zeolite Y supported MgO (denoted as MgO@Y) composites have been successfully prepared using $Mg(NO_3)_2$ as precursor via a facile solid-state heat dispersion approach. The samples are characterized by X-ray diffraction and N_2 adsorption/desorption, and investigated for CO_2 adsorption performance including adsorption capacity, adsorption selectivity and stability. The results reveal that MgO can be highly dispersed on the surfaces of zeolite Y support after the activation at high temperatures, and the monolayer dispersion capacity of MgO on zeolite Y support is 3 mmol/g zeolite Y. The resulting MgO(3.0)@Y adsorbent with the magnesium loadings of 3 mmol/g zeolite Y displays a high CO_2 adsorption capacity of 2.78 mmol/g at 500 kPa, which is about 28% higher than that of zeolite Y support. Moreover, the MgO(3.0)@Y adsorbent displays a high CO_2/N_2 adsorption selectivity of 32 and a excellent cyclic stability. Its good performance as well as its facile preparation process make it attractive candidate for the adsorption of CO_2 in flue gas vents. In addition, the isosteric heat of CO_2 adsorption on the MgO(3.0)@Y sample was calculated from the Clausius–Clapeyron equation, and the values the isosteric heats of adsorption lie in the range of 27.8–20.0 kJ/mol.

Keywords MgO@Y adsorbent · CO_2 · Solid-state heat dispersion · Selectivity · Stability

1 Introduction

Carbon dioxide (CO_2) is the primary greenhouse gas, which is accountable for about two-thirds of greenhouse effect, and the major source of CO_2 emissions is flue gas from coal-fired power plants (Koerner and Klopatek 2002). Therefore, it is urgent to develop the efficient materials and processes for CO_2 removal from flue gases resulting from coal burning for the sustainable environment development. Carbon capture, utilization and sequestration (storage) (CCUS) is the most promising alternative for reducing CO_2 emissions, and CO_2 capture is a critical process (Chu 2009; Hasana et al. 2015).

Currently, proven technologies for the CO_2 capture from flue gases mostly rely on absorption, membrane separation, cryogenic distillation and adsorption (Olajire 2010; Li et al. 2013a; Song et al. 2019). Among them, amine scrubbing is currently the most widely used commercial technology for CO_2 capture. However, it suffers from some disadvantages, including the high energy consumption of regeneration, the equipment corrosion, and the volatility and degradation of solvent (Rao and Rubin 2002). Adsorption processes is considered as a most promising method for replacing the conventional amine absorption technologies due to its low regeneration energy requirements, no liquid waste, and easy operations (Figueroa et al. 2010). For the adsorption separation technology, the moisture and the higher temperature in flue gases could greatly influenced the CO_2 adsorption performance on current adsorbents, and some adsorbents could be easily poisoned and deactivated by gas impurities such as NO_x and SO_x, making it difficulty in industrial application for the CO_2 capture from flue gases. Therefore, the significant research efforts are being undergoing to develop the feasible efficient adsorbents to capture CO_2.

Presently, it has been reported that a variety of solid adsorbents (Wang et al. 2011; Billemont et al. 2017; Rocha et al. 2017; Regufe et al. 2018) including zeolites, activated carbons and metal–organic frameworks (MOFs) display a high adsorption capacity of CO_2. However, activated

✉ Weiwen Wang
wwwang@qust.edu.cn

1 College of Chemical Engineering, Qingdao University of Science and Technology, Qingdao 266042, China

2 Fundamental Chemistry Experiment Center (Gaomi), Qingdao University of Science and Technology, Gaomi 261500, China

carbons always show the low selectivity, and CO_2 adsorption capacities on zeolites and MOFs decrease significantly in the presence of moisture that is essentially present in flue gas, so these absorbents alone are difficult to meet Department of Energy (DoE) requirements of 95% CO_2 purity, 90% recovery for effective CCUS from flue gases with a low energy consumption (Nikolaidis et al. 2018). To achieve high CO_2 capture performance, amine-functionalized adsorbents have been paid great attentions, and mainly prepared by introducing amine functional groups with high affinity for CO_2 onto porous solid materials through a physical impregnation or chemical grafting method (Chen et al. 2014). The prepared composite materials combine the advantages of porous support and amine groups, leading to the enhanced mass transfer, high CO_2 capture capacity, and desirable CO_2 adsorption selectivity. Nonetheless, the mechanical property and thermal stability need to be further improved for amine-based adsorbents.

Recently, adsorbents based on the alkali metals and alkali earth metal oxides have been paid great attentions for the CO_2 capture (Yang et al. 2010; Iruretagoyena et al. 2015; Song et al. 2016; Zhao et al. 2018; Kodasma et al. 2019). Among them, MgO is a promising adsorbent to capture CO_2 owing to its appropriate basic strength and at a moderate operation temperature than that of CaO, and more cost-effective than Li_2O (Jiao et al. 2013; Kim et al. 2014). However, pure MgO exhibits the drawbacks of low surface area and surface formation of a termination layer of carbonate hindering the interaction between MgO and CO_2 (Liu et al. 2008). To overcome these drawbacks, extensive efforts have been devoted to the development of various MgO based porous adsorbents by introducing MgO into porous supports such as molecular sieves (Zukal et al. 2013), Al_2O_3 (Dong et al. 2015), activated carbon (Shahkarami et al. 2016) and TiO_2 (Hiremath et al. 2017), allowing more efficient contact between the MgO and CO_2. For instance, the supported MgO/γ-Al_2O_3 adsorbent achieves a CO_2 adsorption capacity of 0.8 mmol/g at low-temperature of 298 K and 1 bar (Han et al. 2015). Generally, the MgO-loaded porous adsorbents are mainly prepared by impregnating the porous supports with an aqueous solution of magnesium salt, and then calcining magnesium salt to MgO at high temperatures. The MgO-based porous adsorbents prepared with the impregnation method, apart from the intensive preparation processes, always have lower valid MgO loadings owing to the solvent effect. Solid-state heat dispersion is a simple and effective approach to introduce metal salt or metal oxide into the channels of the porous solid materials, and can achieve more valid metal loadings on the surfaces of the supports compared with the conventional impregnation method (Huang et al. 2015; Gao et al. 2016a). And, after activation at high temperatures, the guest species can highly dispersed on the surfaces of the supports. Herein, zeolite Y supported MgO (MgO@Y) for CO_2 capture was prepared by a solid-state heat dispersion method without any solvents and organic templates. The aim of the work is to develop a MgO-based CO_2 adsorbent by a facile preparation method. The obtained adsorbents were investigated for CO_2 adsorption, and their structural and physical properties were characterized by X-ray powder diffraction (XRD) and N_2 adsorption/desorption isotherms. In addition, the CO_2 cyclic stability and the isosteric heat of CO_2 adsorption on the prepared adsorbent were also studied.

2 Experimental

2.1 Materials

$Mg(NO_3)_2{\cdot}6H_2O$ (AR) and Zeolite Y (HY, $SiO_2/Al_2O_3 = 7$, $Na_2O = 0.8\%$) were purchased from Qingdao Zhengye Fine Chemical Research Institute and the Catalyst Plant of Nankai University, respectively. CO_2, N_2 and helium gases were purchased from Qingdao Dehai Gas Co., Ltd. All the gases had purities of or above 99.99%.

2.2 Sample preparation

MgO@Y adsorbents were prepared by a solid-state dispersion method. In a typical run, 3.846 g $Mg(NO_3)_2{\cdot}6H_2O$ (15 mmol) and 5.000 g zeolite Y powder was mixed and grinded for 30 min, and then the mixture was activated at 300 °C for 4 h and 550 °C for 4 h in air. Thereby, the sample with magnesium loadings of 3.0 mmol/g zeolite Y was obtained. According to these steps, the sample with different magnesium loadings of 2.0, 3.0, 4.0 and 5.0 mmol/g zeolite Y were prepared and denoted as $Mg(NO_3)_2$(X)@Y and MgO(X)@Y before and after the activation, where X represents the magnesium loadings in mmol per gram zeolite Y.

2.3 Characterizations

Powder X-ray diffraction patterns were obtained on a Rigaku D/max-2500 diffractometer employing the graphite filtered Cu Kα radiation ($\lambda = 0.154$ nm) in the 2θ ranges from 5° to 80°. Nitrogen adsorption–desorption isotherms of the samples were measured on a Micromeritics ASAP 2020 system at liquid N_2 temperature (77 K). Prior to the measurements, all the samples were evacuated at 573 K for 4 h. The Brunauer–Emmett–Teller (BET) method was utilized to calculate the specific surface areas of the samples from the isotherms. The total pore volumes were estimated from the adsorption equilibrium isotherms at a relative pressure (p/p_0) of 0.99.

2.4 Adsorption measurements

The adsorption isotherms were measured using a static volumetric method (Gao et al. 2016b, c). The apparatus mainly consisted of an adsorption unit, a loading cell, two pressure transducers, a temperature-controlled electric oven, a mechanical vacuum pump. The volumes of the adsorption unit and the loading cell were measured by water filling and the expansion of helium gas, respectively. Before each measurement, 5 g adsorbent inside the adsorption unit was regenerated in situ at 473 K under the vacuum realized by a mechanical pump to remove the gases impurities retained inside. Usually, most of the adsorbent needs to be regenerated for several hours under vacuum or inert gas purge at high temperatures to achieve a complete sample regeneration. In this work, the pressure value of the adsorption unit reached zero in about 5–10 min under the above regeneration condition and remained unchanged for a long time, but 30 min of regeneration time was used to guarantee that the regeneration fully completed. After regeneration, the adsorption unit was cooled down to the set adsorption temperature. The void volume of the adsorption unit was measured by the expansion of helium gas. After that, CO_2 was introduced into the loading cell, and its pressure and temperature were recorded when the values were stabilized. Then the valve connected the adsorption unit and the loading cell was opened, allowing CO_2 to contact with the adsorbents. The pressure value of the adsorption unit and loading cell usually reach a constant value in about 10 min, but 30 min of adsorption time was used for each point to guarantee that the adsorption fully reached to equilibrium. After the pressure value was recorded, the valve was closed and an additional amount of CO_2 was fed into the loading cell, and the same operation was repeated to obtain another adsorption equilibrium point at a higher pressure. The adsorption measurements of CO_2 were carried out at the temperature range of 303 to 333 K and pressures up to 500 kPa. The adsorbed amounts were calculated from the experimental temperatures and pressures using the mass balance equation derived from the equation of state before and after adsorption equilibrium.

2.5 Adsorption theories

2.5.1 Adsorption equilibrium isotherm equations

Many adsorption isotherm models including Langmuir (Langmuir 1918), Freundlich (Freundlich 1906), Sips (Langmuir–Freundlich) (Sips 1948), Toth (Toth 1971), Dual-site Langmuir (DSL) (Kapoor et al. 1990), etc., have been established to investigate the adsorbate-adsorbent interactions. The DSL model, which is an extension of the Langmuir model, is a thermodynamically consistent model, and has been widely used to model the adsorptive processes, especially when the adsorbent surface exhibits a heterogeneous nature. In this study, the DSL model was chosen for correlating the isotherm data as the model is easy to implement in the IAST algorithm with a good accuracy, and is given by

$$q = q_{A,sat}\frac{b_A p}{1 + b_A p} + q_{B,sat}\frac{b_B p}{1 + b_B p}, \tag{1}$$

where q is the adsorption amounts (mmol/g), p is the equilibrium pressure (kPa), and $q_{A,sat}$ and $q_{B,sat}$ are the saturated adsorption amounts of dual sites A and B (mmol/g), respectively. b_A and b_B are the affinity coefficients of sites A and B (kPa^{-1}), respectively, and their temperature dependence are described by

$$b_A = b_{A0}\exp(-\Delta H_A/RT), \tag{2}$$

$$b_B = b_{B0}\exp(-\Delta H_B/RT), \tag{3}$$

where b_{A0} and b_{B0} are the fitting constants, R is the universal gas constant (J mol^{-1} K^{-1}), T is temperature (K), and ΔH is the heat of adsorption (kJ/mol).

2.5.2 Adsorption selectivity

Multi-component adsorption equilibrium data is very important for designing industrial gas adsorption separation processes. However, current measurement techniques have some difficulty in measuring the adsorption equilibrium data for the mixed gases. Therefore, in the past few decades, a series of theoretical models have been developed to predict multi-component adsorption equilibrium data by single-component adsorption data. Although the correlative multi-component prediction models has some limitations (Rao and Sirca 1999; Li and Tezel 2008), they are widely employed to predict multi-component adsorption equilibrium data by pure component adsorption data. Among them, the Ideal Adsorbed Solution Theory (IAST) presented by Myers and Prausnitz (1965) is the most common model, and many studies affirm the accuracy of IAST in providing good mixture adsorption predictions (Wang et al. 2014; Avijegon et al. 2018). In this work, the DSL model was combined with IAST to calculate the adsorption selectivity for the binary mixture. The adsorption selectivity of component 1 over component 2 ($S_{1/2}$) for a binary mixture is commonly defined as (Bahamon and Vega 2016):

$$S_{1/2} = \frac{x_1/x_2}{y_1/y_2}, \tag{4}$$

where x and y represent the mole fractions of components in the adsorbed phase and gas phase, respectively. In this work, components 1 and 2 are CO_2 and N_2, respectively.

2.5.3 Isosteric heat of adsorption

From the adsorption isotherms collected at different temperatures, the isosteric heat of adsorption can be calculated by the Clausius–Clapeyron equation as follows (Choma et al. 2016):

$$Q_{st} = RT^2 \left(\frac{\partial \ln p}{\partial T} \right)_{q_a}, \quad (5)$$

where Q_{st} is the isosteric heat of adsorption (kJ/mol), and q_a is a specific adsorbate loading (mmol/g).

3 Results and discussion

3.1 Characterization of MgO@Y adsorbents

Figure 1 shows the XRD patterns of pure MgO, zeolite Y and the supported $Mg(NO_3)_2$ samples with different magnesium loadings before and after activation at high temperatures. It can be seen that, before activation, the $Mg(NO_3)_2$@Y sample show the diffraction peaks of $Mg(NO_3)_2$ at 2θ values of 15.3°, 20.2°, 21.5°, 27.2° and 30.7° (Ling et al. 2017). After activation, for the MgO@Y samples, only the typical diffraction peaks of zeolite Y are observed, and neither $Mg(NO_3)_2$ nor MgO are observed for the MgO@Y samples, suggesting that MgO is highly dispersed on the surfaces of zeolite Y support. The absence of MgO reflections in XRD patterns might be owing to that the smaller crystallites of highly dispersed MgO are undetectable by XRD (Chen et al. 2010). A high dispersion of the magnesium salts on zeolite Y made the active components of MgO tend to spread rather than agglomerate on the surfaces of support.

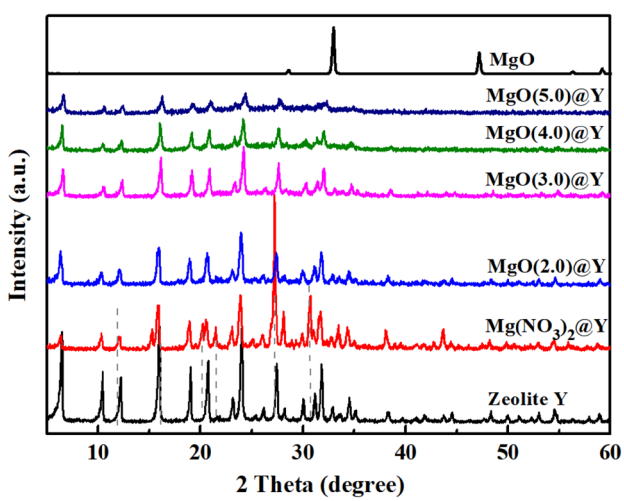

Fig. 1 XRD patterns of MgO, zeolite Y and $Mg(NO_3)_2$ loaded zeolite Y before and after activation

Figure 2 shows the N_2 adsorption–desorption isotherms of zeolite Y support and MgO@Y samples with different magnesium loadings at 77 K. It can be seen that the N_2 adsorption amounts apparently decrease with increasing the magnesium loadings. The BET surface area, pore volume and average pore diameters of zeolite Y support and MgO@Y samples are summarized in Table 1. The specific surface area and pore volume of the samples decrease gradually with the increasing magnesium loadings, resulting from the occupation of the partial surface areas and the pore volumes of zeolite Y by MgO. For the MgO@Y samples, when increasing the magnesium loading from 2.0 to 3.0 mmol/g, the specific surface area and pore volume of the samples decrease slowly, and when further increase the magnesium loadings, these values decrease sharply, indicating that the specific surface area and pore volume of the samples are occupied more seriously by MgO when the magnesium loadings is higher than 3.0 mmol/g. In addition, the average pore diameter of the samples increases with an increase in magnesium loadings. As more micropores are occupied, it results

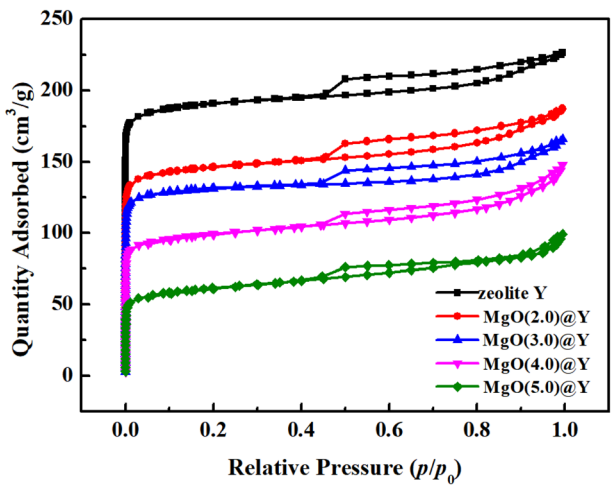

Fig. 2 N_2 adsorption/desorption isotherms at 77 K on zeolite Y and MgO@Y samples with different magnesium loadings

Table 1 Textural properties of zeolite Y and MgO@Y samples

Samples	BET surface area (m^2/g)	Total pore volume (cm^3/g)	Average pore diameter (nm)[a]
Zeolite Y	577	0.35	2.43
MgO(2.0)@Y	435	0.29	2.66
MgO(3.0)@Y	399	0.27	2.71
MgO(4.0)@Y	306	0.23	2.98
MgO(5.0)@Y	193	0.15	3.18

[a]Adsorption average pore diameter (4 V/A by BET)

in an increased average pore sizes because the percentage of the available mesopores in zeolite Y increases (Ramli and Amin 2015).

3.2 Adsorption performance of CO_2 on MgO@Y samples

Figure 3 illustrates the effect of the magnesium loadings on the adsorption performance of CO_2. It can be seen that pure MgO has a low CO_2 adsorption capacity, resulting from the low surface area-to-volume ratio. The support of zeolite Y shows a CO_2 adsorption capacity of 2.18 mmol/g at 500 kPa, caused by the physical interaction between CO_2 and zeolite Y. When introducing MgO, the MgO@Y samples show the higher adsorption capacities compared to the zeolite Y support, implying that the introduction of MgO on zeolite Y is crucial to obtain adsorbents with high CO_2 adsorption capacity. When the magnesium loadings increase to 3.0 mmol/g zeolite Y, the CO_2 adsorption amounts at 500 kPa increase from 2.18 to 2.78 mmol/g. When the magnesium loadings further increase to 5.0 mmol/g zeolite Y, the CO_2 adsorption capacity decreases gradually. This may be due to the accumulation of excessive MgO on the surfaces of samples, resulting in the decrease of the effective active sites and the blockage of pore channels. The results indicate that the monolayer dispersion capacity of MgO on zeolite Y is 3 mmol/g. When the magnesium loadings is higher than 3 mmol/g, the excess magnesium species may cumulate on the monolayer, which is in good agreement with N_2 adsorption–desorption results. In addition, it can been that the CO_2 adsorption capacities of all the MgO@Y samples are higher than that of the zeolite Y support at low pressures, and the CO_2 adsorption amounts on MgO(3.0)@Y at 20 kPa increase from 0.15 to 0.35 mmol/g, ascribed to the occupation of the partial pore volumes and surface areas of the zeolite Y support by MgO, resulting in that the physical absorption sites for CO_2 on the adsorbents is gradually replaced by the chemical adsorption between MgO on the adsorbents with CO_2 molecules with increasing the magnesium loadings.

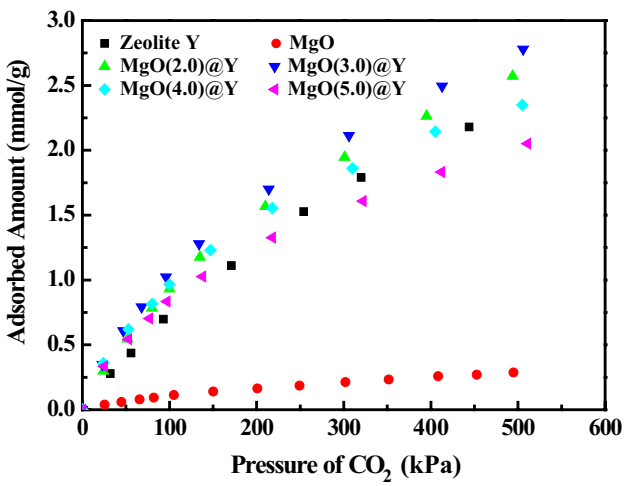

Fig. 3 Adsorption isotherms of CO_2 on MgO, zeolite Y and the MgO@Y adsorbents with different magnesium loadings at 303 K

For the adsorption separation of CO_2 from gas mixtures, besides adsorption capacity, the adsorption selectivity is also a key factor for the separation performance. Figure 4a gives the experimental and correlated adsorption isotherms of pure CO_2 and N_2 on the MgO(3.0)@Y adsorbent at 303 K, and the DSL fitting parameters are listed in Table 2. It can be seen that the adsorption capacity of CO_2 on MgO(3.0)@Y is significantly higher than that of N_2, which is ascribed to the stronger interaction between the highly dispersed MgO on the adsorbent and CO_2 and the weaker van der Waals and electrostatic interactions of N_2 with the adsorbent. Based on the single gas adsorption isotherms, the CO_2/N_2 adsorption selectivity were predicted by IAST for the binary mixture

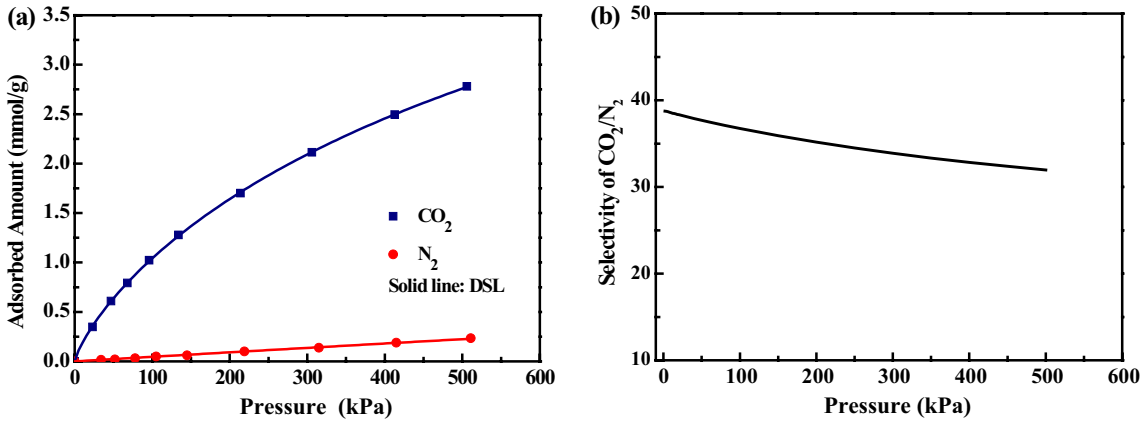

Fig. 4 Adsorption isotherms of CO_2 and N_2 on MgO(3.0)@Y at 303 K (**a**) and IAST-predicted CO_2/N_2 adsorption selectivity for the binary mixture with CO_2/N_2 molar ratio of 15:85 (**b**)

Table 2 Dual-site Langmuir (DSL) fitting parameters for CO_2 and N_2 adsorption on MgO(3.0)@Y

Parameters	$q_{A,sat}$ (mmol/g)	b_{A0} (kPa^{-1})	$-\Delta H_A$ (kJ/mol)	$q_{B,sat}$ (mmol/g)	b_{B0} (kPa^{-1})	$-\Delta H_B$ (kJ/mol)	b_A (kPa^{-1})	b_B (kPa^{-1})
CO_2	0.82	6.17×10^{-6}	19.6	5.93	8.55×10^{-7}	17.9	–	–
N_2	0.82	–	–	5.93	–	–	6.88×10^{-5}	6.89×10^{-5}

with CO_2/N_2 molar ratio of 15:85, which is the typical component of flue gases in a coal fired power plant, and depicted in Fig. 4b. It can be seen that the CO_2/N_2 adsorption selectivity decreases gradually from 39 to 32 with an increase in adsorption pressure, and at a given pressure of 100 kPa, the CO_2/N_2 adsorption selectivity is as high as 37. In addition, the CO_2/N_2 adsorption selectivity of the prepared MgO(3.0)@Y adsorbent was compared with that of common porous materials, such as MOFs, carbon materials and zeolites, and the comparison results are summarized in Table 3. Overall, in Table 3, MOFs has higher CO_2/N_2 adsorption selectivity than carbon materials and zeolites, however, MOFs always suffer from the expensive cost, durability and mechanical strength problems, limiting its industrial application (Lee and Park 2015). In comparison, the MgO(3.0)@Y adsorbent in this work exhibits a higher CO_2/N_2 adsorption selectivity than other adsorbents except for zeolite 13X in Table 3, and the CO_2/N_2 adsorption selectivity of MgO(3.0)@Y adsorbent is almost 3.7 times of that of zeolite Y, implying that the introducing of MgO onto the zeolite Y support is crucial to obtain adsorbents with a high CO_2/N_2 adsorption selectivity. For the zeolite 13X adsorbent, the CO_2/N_2 adsorption selectivity was greatly influenced by the adsorption pressure, and decreased significantly to ~5 at 500 kPa (Belmabkhout and Sayari 2009), which was lower than that of 32 of MgO(3.0)@Y in this work. The higher CO_2/N_2 adsorption selectivity suggests that the MgO(3.0)@Y adsorbent can preferentially adsorb CO_2 over N_2 in a binary mixture of CO_2/N_2.

For potential application, an ideal adsorbent should not only display the high adsorption capacity and high adsorption selectivity, but also exhibit a good cyclic stability performance. Thus, the adsorption/desorption cycles with the adsorption at 303 K and desorption at 473 K for 30 min under vacuum were repeated for ten times on MgO(3.0)@Y, and the result is depicted in Fig. 5a. It can be seen that, in the ten adsorption/desorption cycles, the CO_2 adsorption capacities are nearly identical. In addition, to mimic a vacuum pressure swing adsorption (VPSA) process, the adsorption/desorption cycles with the adsorption and desorption at the same temperature of 303 K were repeated for five times on MgO(3.0)@Y. The results in Fig. 5b show that the CO_2 adsorption capacities are nearly identical in the five cycles at the operation temperature of 303 K, and the reversible CO_2 adsorption capacity is 2.46 mmol/g, which is close to that of 2.78 mmol/g with the desorption at 473 K. The result implies that the adsorbed CO_2 on MgO(3.0)@Y could be desorbed at ambient temperature under vacuum, which is attributed to the relatively low isosteric heat of CO_2 adsorption on the MgO(3.0)@Y sample (see Fig. 6). The results indicate that the adsorbent displays a good cyclic stability for CO_2 adsorption, demonstrating that this adsorbent can

Table 3 Comparison of CO_2/N_2 selectivity at 100 kPa and heat of adsorption of CO_2 adsorption on different adsorbents

Adsorbent	CO_2/N_2 selectivity	Q_{st} (kJ/mol)	References
UTSA-16	262 (296 K)	34.6	Xiang et al. (2012)
Mg-MOF-74	182 (298 K)	47	Xiang et al. (2012), Herm et al. (2011)
Cu-BTC	~50 (298 K)	~25	Wu et al. (2019)
Ni-MOF-74	30 (298 K)	42	Dietzel et al. (2009)
rht-MOF-7	25 (303 K)	45–25	Luebke et al. (2012)
MIL-101	11.43 (298 K)	44	Lin et al. (2013)
AC-1	9 (298 K)	20	Sevilla and Fuertes (2011)
AC-2	7.9 (298 K)	24–25	Li et al. (2015)
Carbon nanotubes	9.7 (300 K)	–	Razavi et al. (2011)
Carbon molecular sieves	6.6 (294 K)	26.5	Carruthers et al. (2012)
Zeolite 13X	~300 (298 K)	20–47	Wilkins and Rajendran (2019)
Na-4A	18.8 (298 K)	~25	Akten et al. (2003)
MCM-41	11 (298 K)	20–25	Belmabkhout and Sayari (2009)
ZSM-5	~8 (298 K)	–	Hefti et al. (2015)
Zeolite Y	~10 (303 K)	25	Pires et al. (1993), Shao et al. (2009)
MgO(3.0)@Y	37 (303 K)	20–39	This work

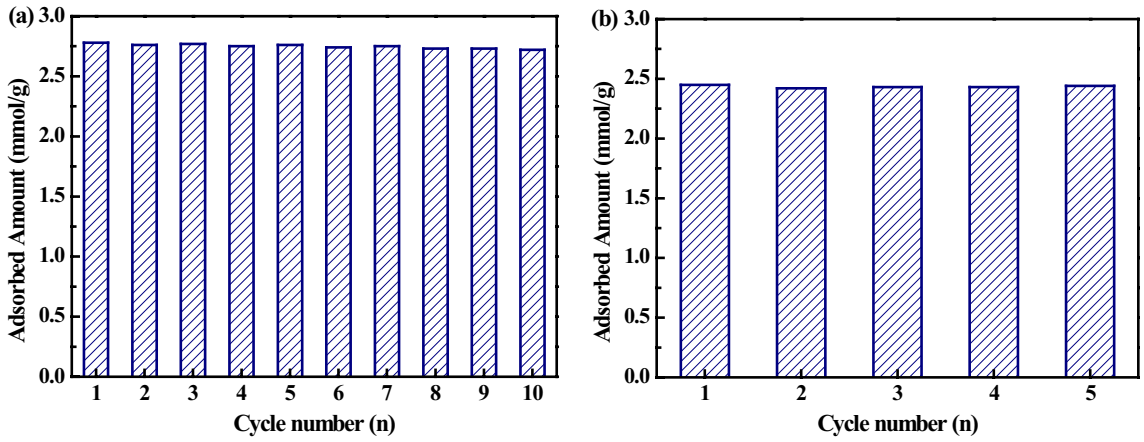

Fig. 5 The cyclic CO_2 adsorption capacity at 500 kPa on MgO(3.0)@Y with the adsorption at 303 K and desorption at 473 K (**a**), and with the adsorption and desorption at 303 K (**b**)

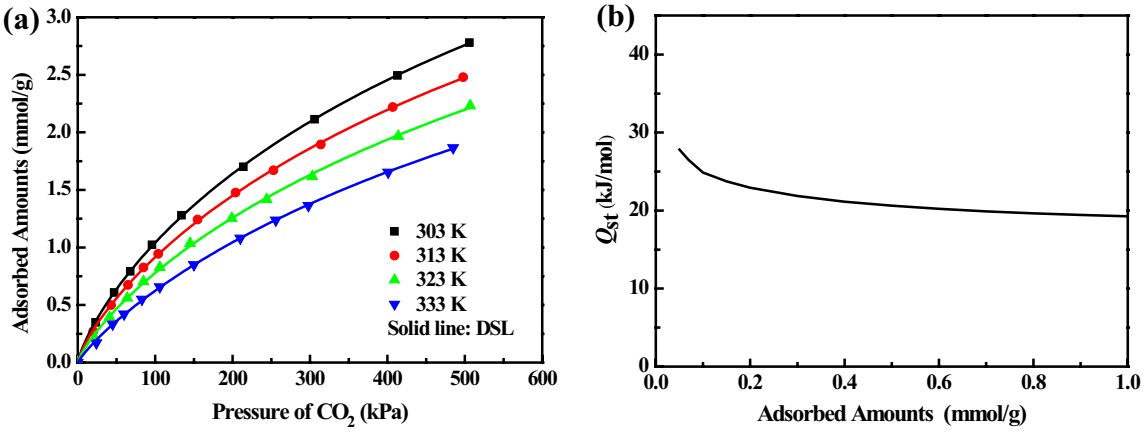

Fig. 6 CO_2 adsorption isotherms at different temperatures (**a**) and isosteric heats of CO_2 adsorption (**b**) on MgO(3.0)@Y sample

be repeatedly used for the CO_2 adsorption and desorption in CO_2 separation processes with the CO_2 adsorption capacity being not changed.

The above results indicate that the prepared MgO@Y adsorbent with a high CO_2 adsorption capability, high adsorption selectivity and good stability is a promising adsorbent for the effective separation of CO_2 from gas mixtures.

Isosteric heat of adsorption is an important parameter for investigating the interactions between adsorbate and adsorbent, and providing useful information to design and operate the practical adsorption process. In this work, CO_2 adsorption isotherms at different temperatures (303 K, 313 K, 323 K and 333 K) presented in Fig. 6a were used to calculate the isosteric heat of CO_2 adsorption on MgO(3.0)@Y sample. The DSL models were used to correlate the experimental data, and the fitting parameters are listed in Table 2. According to Eq. (5), the isosteric heats of adsorption as a function of the CO_2 loading were calculated, and depicted in Fig. 6b. From Fig. 6a, the CO_2 adsorption capacity decreases with increasing the adsorption temperatures, indicating that the CO_2 adsorption on MgO(3.0)@Y is an exothermic process. From Fig. 6b, the isosteric heats of CO_2 adsorption on MgO(3.0)@Y decrease gradually from 27.8 to 20.0 kJ/mol with increasing the CO_2 adsorption amounts to 1.0 mmol/g. This variation may be associated with the heterogeneity of surface property for the material. The calculated isosteric heat value of adsorption and the variation is similar to that on MgO/C adsorbent obtained by Li et al. (2013b). This relatively low isosteric heat, which is slightly higher than that of zeolite Y (see Table 3), suggests that the interaction strength between CO_2 and MgO-based adsorbents is relatively weaker than the strong acid–base interactions, resulting in a moderate operation temperature for CO_2 capture and a low regeneration energy consumption using MgO-based adsorbents.

4 Conclusions

A series of zeolite Y supported MgO (MgO@Y) adsorbents for selective adsorption for CO_2 has been successfully prepared using $Mg(NO_3)_2$ as precursor via a facile solid-state heat dispersion approach without any solvents and organic templates. $Mg(NO_3)_2$ supported on zeolite Y can be converted to highly dispersed MgO after activation at high temperatures. The obtained MgO@Y sample with the magnesium loading of 3 mmol/g zeolite Y achieves a high CO_2 adsorption capacity of 2.78 mmol/g and a high CO_2/N_2 adsorption selectivity of 32 at 303 K and 500 kPa. In addition, this adsorbent also shows an excellent cyclic stability in ten adsorption/desorption cycles for CO_2. The MgO(3.0)@Y adsorbent with good CO_2 adsorption capacity, good adsorption selectivity, and excellent cyclic stability as well as its facile preparation process shows an attractive candidate for CO_2 capture from flue gas vents.

Acknowledgements This work has been supported by Natural Science Foundation of Shandong Province (No. ZR2018BB071).

Compliance with ethical standards

Conflict of interest The authors declare that they have no conflict of interest.

Ethical approval This work does not contain any studies with human participants or animals performed by any of the authors.

References

Akten, E.D., Siriwardane, R., Sholl, D.S.: Monte carlo simulation of single- and binary-component adsorption of CO_2, N_2, and H_2 in Zeolite Na-4A. Energ. Fuel. **17**, 977–983 (2003)

Avijegon, G., Xiao, G., Li, G., May, E.F.: Binary and ternary adsorption equilibria for $CO_2/CH_4/N_2$ mixtures on Zeolite 13× beads from 273 to 333 K and pressures to 900 kPa. Adsorption **24**(4), 381–392 (2018)

Bahamon, D., Vega, L.F.: Systematic evaluation of materials for post-combustion CO_2 capture in a temperature swing adsorption process. Chem. Eng. J. **284**, 438–447 (2016)

Belmabkhout, Y., Sayari, A.: Adsorption of CO_2 from dry gases on MCM-41 silica at ambient temperature and high pressure. 2: adsorption of CO_2/N_2, CO_2/CH_4 and CO_2/H_2 binary mixtures. Chem. Eng. Sci. **64**, 3729–3735 (2009)

Billemont, P., Heymans, N., Normand, P., Weireld, G.D.: IAST predictions vs co-adsorption measurements for CO_2 capture and separation on MIL-100 (Fe). Adsorption **23**(2–3), 225–237 (2017)

Carruthers, J.D., Petruska, M.A., Sturm, E.A., Wilson, S.M.: Molecular sieve carbons for CO_2 capture. Microporous Mesoporous Mater. **154**, 62–67 (2012)

Chen, Y., Xie, C., Li, Y., Song, C., Bolin, T.B.: Sulfur poisoning mechanism of steam reforming catalysts: an X-ray absorption near edge structure (XANES) spectroscopic study. Phys. Chem. Chem. Phys. **12**(21), 5707–5711 (2010)

Chen, C., Kim, J., Ahn, W.S.: CO_2 capture by amine-functionalized nanoporous materials: a review. Korean J. Chem. Eng. **31**(11), 1919–1934 (2014)

Choma, J., Stachurska, K., Marszewski, M., Jaroniec, M.: Equilibrium isotherms and isosteric heat for CO_2 adsorption on nanoporous carbons from polymers. Adsorption **22**(4), 581–588 (2016)

Chu, S.: Carbon capture and sequestration. Science **325**(5948), 1599 (2009)

Dietzel, P.D.C., Besikiotis, V., Blom, R.: Application of metal-organic frameworks with coordinatively unsaturated metal sites in storage and separation of methane and carbon dioxide. J. Mater. Chem. **19**, 7362–7370 (2009)

Dong, W., Chen, X., Yu, F., Wu, Y.: $Na_2CO_3/MgO/Al_2O_3$ solid sorbents for low-temperature CO_2 capture. Energy Fuel. **29**(2), 968–973 (2015)

Figueroa, J.D., Fout, T., Plasynski, S., McIlvried, H.: Advances in CO_2 capture technology—The U.S. Department of Energy's Carbon Sequestration Program. Int. J. Greenh. Gas Con. **2**(1), 9–20 (2008)

Freundlich, H.M.F.: Over the adsorption in solution. J. Phys. Chem. **57**, 385–471 (1906)

Gao, F., Wang, Y., Wang, X., Wang, S.: Selective CO adsorbent CuCl/AC prepared using $CuCl_2$ as a precursor by a facile method. RSC Adv. **6**(41), 34439–34446 (2016a)

Gao, F., Wang, Y., Wang, S.: Selective adsorption of CO on CuCl/Y adsorbent prepared using $CuCl_2$ as precursor: equilibrium and thermodynamics. Chem. Eng. J. **290**, 418–427 (2016b)

Gao, F., Wang, Y., Wang, X., Wang, S.: Ethylene/ethane separation by Cu/AC adsorbent prepared using $CuCl_2$ as a precursor. Adsorption **22**(7), 1013–1022 (2016c)

Han, S.J., Bang, Y., Lee, H., Lee, K., Song, I.K., Seo, J.G.: Synthesis of a dual-templated MgO-Al_2O_3 adsorbent using block copolymer and ionic liquid for CO_2 capture. Chem. Eng. J. **270**, 411–417 (2015)

Hasana, M.M.F., First, E.L., Boukouvala, F., Flouda, C.A.: A multi-scale framework for CO_2 capture, utilization, and sequestration: CCUS and CCU. Comput. Chem. Eng. **81**, 2–21 (2015)

Hefti, M., Marx, D., Joss, L., Mazzotti, M.: Adsorption equilibrium of binary mixtures of carbon dioxide and nitrogen on zeolites ZSM-5 and 13X. Microporous Mesoporous Mater. **215**, 215–222 (2015)

Herm, Z.R., Swisher, J.A., Smit, B., Krishna, R., Long, J.R.: Metal-organic frameworks as adsorbents for hydrogen purification and precombustion carbon dioxide capture. J. Am. Chem. Soc. **133**, 5664–5667 (2011)

Hiremath, V., Shavi, R., Seo, J.G.: Controlled oxidation state of Ti in MgO-TiO_2 composite for CO_2 capture. Chem. Eng. J. **308**, 177–183 (2017)

Huang, Y., Tao, Y., He, L., Duan, Y., Xiao, J., Li, Z.: Preparation of CuCl@AC with high CO adsorption capacity and selectivity from CO/N_2 binary mixture. Adsorption **21**(5), 373–381 (2015)

Iruretagoyena, D., Huang, X., Shaffer, M.S.P., Chadwick, D.: Influence of alkali metals (Na, K, and Cs) on CO_2 adsorption by layered double oxides supported on graphene oxide. Ind. Eng. Chem. Res. **54**(46), 11610–11618 (2015)

Jiao, X., Li, L., Zhao, N., Xiao, F., Wei, W.: Synthesis and low-temperature CO_2 capture properties of a novel Mg-Zr solid sorbent. Energy Fuel. **27**(9), 5407–5415 (2013)

Kapoor, A., Ritter, J.A., Yang, R.T.: An extended langmuir model for adsorption of gas mixtures on heterogeneous surfaces. Langmuir **6**(3), 660–664 (1990)

Koerner, B., Klopatek, J.: Anthropogenic and natural CO_2 emission sources in an arid urban environment. Environ. Pollut. **116**, S45–S51 (2002)

Kodasma, R., Fermoso, J., Sanna, A.: Li-LSX-zeolite evaluation for post-combustion CO_2 capture. Chem. Eng. J. **358**, 1351–1362 (2019)

Kim, K., Han, J.W., Lee, K.S., Lee, W.B.: Promoting alkali and alkaline-earth metals on MgO for enhancing CO_2 capture by first-principles calculations. Phys. Chem. Chem. Phys: PCCP **16**(45), 24818–24823 (2014)

Langmuir, I.: The adsorption of gases on plane surfaces of glass, mica and platinum. J. Am. Chem. Soc. **40**, 1361–1403 (1918)

Lee, S.Y., Park, S.J.: A review on solid adsorbents for carbon dioxide capture. J. Ind. Eng. Chem. **23**, 1–11 (2015)

Li, P., Tezel, F.H.: Pure and binary adsorption equilibria of carbon dioxide and nitrogen on silicalite. J. Chem. Eng. Data **53**, 2479–2487 (2008)

Li, B., Duan, Y., Luebke, D., Morreale, B.: Advances in CO_2 capture technology: a patent review. Appl. Energy **102**, 1439–1447 (2013a)

Li, Y.Y., Han, K.K., Lin, W.G., Wan, M.M., Wang, Y., Zhu, J.H.: Fabrication of a new MgO/C sorbent for CO_2 capture at elevated temperature. J. Mater. Chem. A **1**(41), 12919–12925 (2013b)

Li, D., Tian, Y., Li, L., Li, J., Zhang, H.: Production of highly microporous carbons with large CO_2 uptakes at atmospheric pressure by KOH activation of peanut shell char. J. Porous Mater. **22**, 1581–1588 (2015)

Lin, Y., Yan, Q., Kong, C., Chen, L.: Polyethyleneimine incorporated metal-Organic frameworks adsorbent for highly selective CO_2 capture. Sci. Rep. **3**, 1859–1865 (2013)

Ling, Z., Liu, J., Wang, Q., Lin, W., Fang, X., Zhang, Z.: $MgCl_2{\cdot}6H_2O$-$Mg(NO_3)_2{\cdot}6H_2O$ eutectic/SiO_2 composite phase change material with improved thermal reliability and enhanced thermal conductivity. Sol. Energy Mater. Sol. C **172**, 195–201 (2017)

Liu, S., Zhang, X., Li, J., Zhao, N., Wei, W., Sun, Y.: Preparation and application of stabilized mesoporous MgO-ZrO_2 solid base. Catal. Commun. **9**(7), 1527–1532 (2008)

Luebke, R., Eubank, J.F., Cairns, A.J., Belmabkhout, Y., Wojtas, L., Eddaoudi, M.: The unique rht-MOF platform, ideal for pinpointing the functionalization and CO_2 adsorption relationship. Chem. Commun. **48**, 1455–1457 (2012)

Myers, A.L., Prausnitz, J.M.: Thermodynamics of mixed-gas adsorption. AIChE J. **11**(1), 121–127 (1965)

Nikolaidis, G.N., Kikkinides, E.S., Georgiadis, M.C.: A model-based approach for the evaluation of new zeolite 13X-based adsorbents for the efficient post-combustion CO_2 capture using P/VSA processes. Chem. Eng. Res. Des. **131**, 362–374 (2018)

Olajire, A.A.: CO_2 capture and separation technologies for end-of-pipe applications: a review. Energy **35**(6), 2610–2628 (2010)

Pires, J., de Carvalho, M.B., Ramoa Ribeiro, F., Derouane, E.G.: Carbon dioxide in Y and ZSM-20 zeolites: adsorption and infrared studies. J. Mol. Catal. **85**, 295–303 (1993)

Ramli, N.A.S., Amin, N.A.S.: Fe/HY zeolite as an effective catalyst for levulinic acid production from glucose: characterization and catalytic performance. Appl. Catal. B **163**, 487–498 (2015)

Rao, M.B., Sirca, S.: Thermodynamic consistency for binary gas adsorption equilibria. Langmuir **15**, 7258–7267 (1999)

Rao, A.B., Rubin, E.S.: A technical, economic and environmental assessment of amine based CO_2 capture technology for power plant greenhouse gas control. Environ. Sci. Technol. **36**(20), 4467–4475 (2002)

Razavi, S.S., Hashemianzadeh, S.M., Karimi, H.: Modeling the adsorptive selectivity of carbon nanotubes for effective separation of CO_2/N_2 mixtures. J. Mol. Model. **17**, 1163–1172 (2011)

Regufe, M.J., Ferreira, A.F.P., Loureiro, J.M., Shi, Y., Rodrigues, A., Ribeiro, A.M.: New hybrid composite honeycomb monolith with 13× zeolite and activated carbon for CO_2 capture. Adsorption **24**(3), 249–265 (2018)

Rocha, L.A.M., Anne Andreassen, K., Grande, C.A.: Separation of CO_2/CH_4 using carbon molecular sieve (CMS) at low and high pressure. Chem. Eng. Sci. **164**, 148–157 (2017)

Sevilla, M., Fuertes, A.B.: Sustainable porous carbons with a superior performance for CO_2 capture. Energy Environ. Sci. **4**, 1765–1771 (2011)

Shahkarami, S., Dalai, A.K., Soltan, J.: Enhanced CO_2 adsorption using MgO-impregnated activated carbon: Impact of preparation techniques. Ind. Eng. Chem. Res. **55**(20), 5955–5956 (2016)

Shao, W., Zhang, L., Li, L., Lee, R.L.: Adsorption of CO_2 and N_2 on synthesized NaY zeolite at high temperatures. Adsorption **15**, 497–505 (2009)

Sips, R.: On the structure of a catalyst surface. J. Chem. Phys. **16**, 490–495 (1948)

Song, G., Zhu, X., Chen, R., Liao, Q., Ding, Y.D., Chen, L.: An investigation of CO_2 adsorption kinetics on porous magnesium oxide. Chem. Eng. J. **283**, 175–183 (2016)

Song, C., Liu, Q., Deng, S., Li, H., Kitamura, Y.: Cryogenic-based CO_2 capture technologies: state-of-the-art developments and current challenges. Renew. Sust. Energ. Rev. **101**, 265–278 (2019)

Toth, J.: State equations of the solid gas interface layer. Acta Chem. Acad. Hung. **69**, 311–317 (1971)

Wang, Q., Luo, J.Z., Zhou, Z.Y., Borgna, A.: CO_2 capture by solid adsorbents and their applications: current status and new trends. Energ. Environ. Sci. **4**(1), 42–55 (2011)

Wang, C., Li, L., Tang, S., Zhao, X.: Enhanced uptake and selectivity of CO_2 Adsorption in a hydrostable metal-organic frameworks via incorporating methylol and methyl groups. ACS Appl. Mater. Interfaces **6**, 16932–16940 (2014)

Wilkins, N.S., Rajendran, A.: Measurement of competitive CO_2 and N_2 adsorption on Zeolite 13X for post-combustion CO_2 capture. Adsorption **25**, 115–133 (2019)

Wu, Y., Lv, Z., Zhou, X., Peng, J., Tang, Y., Li, Z.: Tuning secondary building unit of Cu-BTC to simultaneously enhance its CO_2 selective adsorption and stability under moisture. Chem. Eng. J. **355**, 815–821 (2019)

Xiang, S., He, Y., Zhang, Z., Wu, H., Zhou, W., Krishna, R., Chen, B.: Microporous metal-organic framework with potential for carbon dioxide capture at ambient conditions. Nat. Commun. **3**, 954–962 (2012)

Yang, S.T., Kim, J., Ahn, W.S.: CO_2 adsorption over ion-exchanged zeolite beta with alkali and alkaline earth metal ions. Microporous Mesoporous Mater. **135**(1–3), 90–94 (2010)

Zhao, B., Ma, L., Shi, H., Liu, K., Zhang, J.: Calcium precursor from stirring processes at room temperature for controllable preparation of nano-structure CaO sorbents for high temperature CO_2 adsorption. J. CO2 Util. **25**, 315–322 (2018)

Zukal, A., Pastva, J., Čejka, J.: MgO-modified mesoporous silicas impregnated by potassium carbonate for carbon dioxide adsorption. Microporous Mesoporous Mater. **167**, 44–50 (2013)